

CONFERENCE PRE-PRINT**OPERATIONAL SPACE OF SMALL ELM AND ELM-FREE REGIMES ON HL-3 TOKAMAK**

N. Wu, K.Y. Yi, Y. R. Zhu, W.C. Wang, Y. He, Z.H. Huang, G. L. Xiao, A. S. Liang, W. Zhao, R. Ke, L.W. Yan, Z.B. Shi, W.L. Zhong
 Southwestern Institute of Physics
 Chengdu, People's Republic of China
 Email: wuna@swip.ac.cn

J. Chen, J. Cheng

Institute of Fusion Science, School of Physical Science and Technology, Southwest Jiaotong University
 Chengdu, People's Republic of China

Abstract

The small ELM and ELM-free H-mode have been achieved on HL-3. The statistical results show that high triangularity favors the ELM-free H-mode, Weak particle transport is observed during the ELM-free sustainment in low q_{95} case, which is accompanied by large scale electromagnetic coherent perturbation; While the high q_{95} and high density benefit another type of ELM-free with strong particle transport accompanied by QCM with the frequency of 20 kHz in the pedestal. Small ELMs have been obtained by increasing density in high triangularity, which is accompanied by a coherent perturbation with a frequency of 6-13 kHz in the pedestal, similar to QCE mechanism. The statistical results show that the high triangularity, high density and high q_{95} favor small ELMs, which provides the reference on the small ELM operation for future fusions.

1. INTRODUCTION

High confinement mode (H-mode) with type-I ELMs will pose unacceptable transient heat fluxes on the divertor target, lead to excessive impurity production, thus it must be controlled or replaced by small ELMs in ITER and future fusion reactors [1]. Natural small ELMs and ELM-free are promising operation regimes in future fusion reactors, such as grassy ELMs achieved on JT-60U [2], EAST [3] and JET [4]; type-II ELMs[5] or quasi-continuous exhaust (QCE) regime obtained on ASDEX upgrade [6, 7]; type-V ELMs observed on NSTX[8] and baseline small ELMs (BSEs) on JET[9]. Grassy ELMs show a dependence on high poloidal β_p , high triangularity δ and high q_{95} , what is more, the counter-NBI also benefits the grassy ELMs observed on JT-60U [10], while on JET, the high internal inductance l_i is found important as well in achieving the grassy ELM[4]. Type-II/QCE is more easily obtained in high density discharge with larger triangularity and elongation, and the resistive ballooning mode at the bottom of pedestal is considered to be responsible for the small ELM burst [7]. Enhanced D-alpha (EDA) regime obtained on Alcator C-Mod [9] is a ELM-free regime, which can be obtained by fueling in high triangularity on ASDEX upgrade[11], and the strong particle transport during the ELM-free is attributed to quasi-coherent mode (QCM) in pedestal. What is more, Super QH-mode was obtained on DIII-D, which has low pedestal collisionality and high confinement level. X-point radiator (XPR) mechanism obtained on ASDEX upgrade has fine core-edge integration performance[12].

HL-3 has the ability of high current and high beta operation [13]. In recent experiments, H-mode with plasma current of 1.5 MA has been obtained, and H-mode with snowflake divertor configuration in 0.5 MA is performed successfully as well. Various H-mode operation regimes are achieved, including type-I, type-III, and small ELMs or ELM-free regimes (QCE, grassy ELM, EDA and so on), which can be compatible with high beta. The small ELM shows a strong dependence on some plasma parameters. In this work, it is focused on small ELM and ELM-free regimes, aiming to explore the physical law on HL-3. The exploration of the operational space for small ELMs and ELM-free regimes with high operational parameters on HL-3 could provide direct reference for the burning plasma in future fusion reactors. This paper is organized as follows: The experiment set-up is provided in section 2; Section 3 presents the main experimental results, including small ELM and ELM-free regimes; Section 4 provides a summary.

2. EXPERIMENTAL SETUP

HL-3 is a tokamak with major radius of $R=1.78$ m and minor radius of $a=0.65$ m, which has ability of high parameter operation with plasma current of 2.5-3 MA, and the toroidal magnetic field of 2.2-3 T. The auxiliary heating reached recently: neutral beam injection $P_{NBI} > 4$ MW, lower hybrid wave $P_{LHW} \sim 1$ MW and electron cyclotron resonance heating $P_{ECRH} \sim 2.5$ MW. It features flexible plasma configuration operation ability, including large elongation $\kappa \leq 1.8$, positive and negative triangularity, which provides superior platform for

achieving different H-mode operational regimes. The critical pedestal diagnostic includes frequency modulated continuous wave (FMCW) reflectometer used to measure density profiles, and charge exchange recombination spectrum (CXRS) and electron cyclotron emission (ECE) are used for the measurements of ion and electron temperature profiles, respectively, which are installed at the mid-plane. The Thomson scattering system could provide the whole profile of the electron density and temperature as well. Doppler backward scattering (DBS) and Beam Emission Spectroscopy (BES) are used to measure the turbulence at the pedestal. The divertor probe array could provide the saturation ion current and heat flux distribution[14]. The stored energy and beta are measured by diamagnetic measurement system. Divertor D_α monitor is used to measure the D_α emission.

3. EXPERIMENTAL RESULTS

Small ELM and ELM-free regimes have been obtained recently on HL-3 with plasma current $I_p = 0.3-1.5$ MA, toroidal Bt = 0.6-1.7 T and toroidal beta $\beta_N > 4$. ELM behaviors varied under different parameters, such as plasma current I_p , electron density n_e , edge safety factor q_{95} , β_N , β_p and plasma configuration parameters, and the results show that 1) the ELM-free regime exhibits a strong dependence on the upper-triangularity δ_u ; 2) Elevated density n_e and enhanced q_{95} promote the suppression of large-amplitude ELMs, achieving small ELMs in moderate-to-high upper-triangularity configurations.

3.1. ELM-free operational regimes

Fig. 1 presents statistical analysis of the parametrical dependence between ELM-free operational and upper-triangularity. The ELMy H-mode usually occurs when the upper-triangularity is low, as marked by the blue diamonds in Fig. 1, but there is a transition to the ELM-free regime when the upper-triangularity exceeds critical threshold, as indicated by the red circles. This law is suitable for different current platform discharges. While if the triangularity is too large, more heating power is required to sustain the H-mode, suggesting a high power threshold of L-H transition requirement.

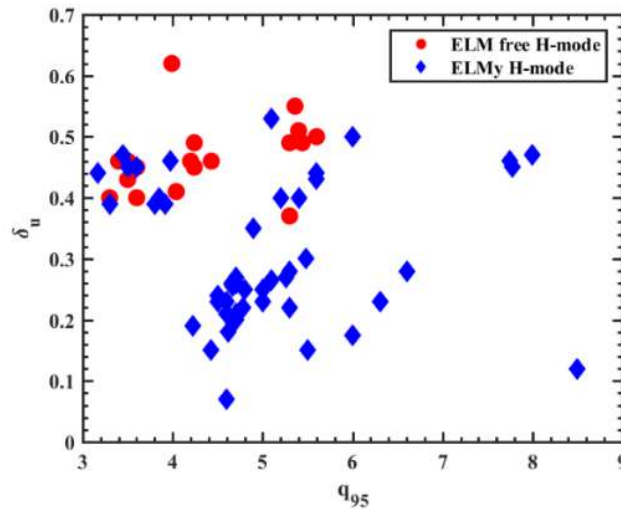


FIG. 1 The dependence of ELM-free regime on triangularity shown by the statistical results, each datum represents one shot discharge.

What is more, two types of ELM-free regimes are observed, one is dominated by electromagnetic coherent perturbation, which usually occurs in low q_{95} , as shown in Fig.2, there is a transition from L-mode to ELM-free H-mode at $t=1550$ ms, and a coherent perturbation with frequency of about 50 kHz appear in the Mirnov signal, and the toroidal number is $n=1$. Besides, the coherent perturbation is also observed in the saturation ion current on the inner divertor, which suggests it is a large scale MHD. This ELM-free regime usually does not induce large transport, thus the density ramp-up rapidly, and terminated with a large ELM or discharge disruption. Another type of ELM-free usually occurs in high density and high q_{95} , which is accompanied by QCM with frequency of about 20 kHz, as displayed in Fig.3, and it is measured by both DBS and BES in pedestal region. This ELM-free

regime is accompanied by enhanced particle transport, which is helpful to the sustainment of ELM-free. Further analysis on the nature of QCM is ongoing.

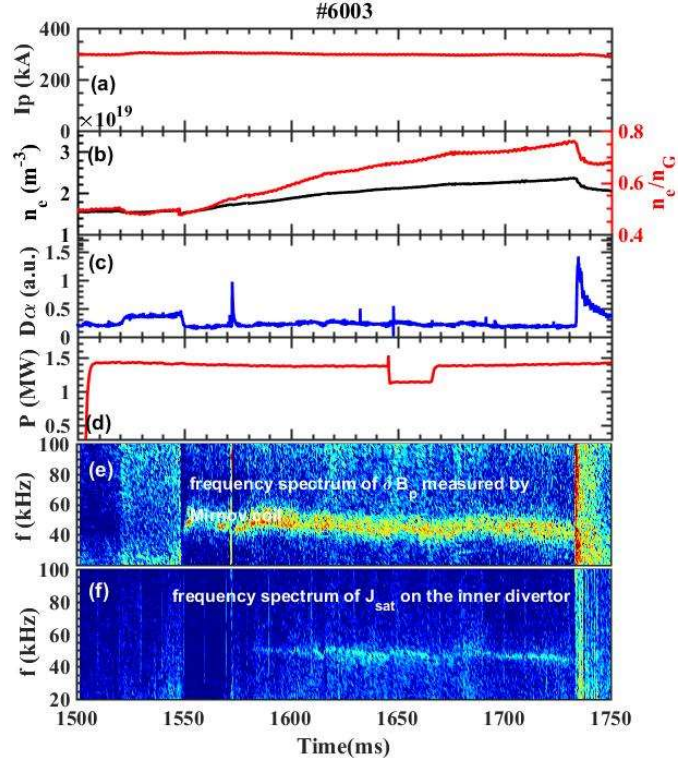


FIG. 2 The ELM-free regime in low q_{95} : (a) plasma current, (b) line-averaged density and normalized density by GreenWald density, (c) divertor D_α emission, (d) NBI power, (e) frequency spectrum of poloidal magnetic perturbation measured by Mirnov coil, (f) frequency spectrum of saturation ion current at the high field side of the divertor.

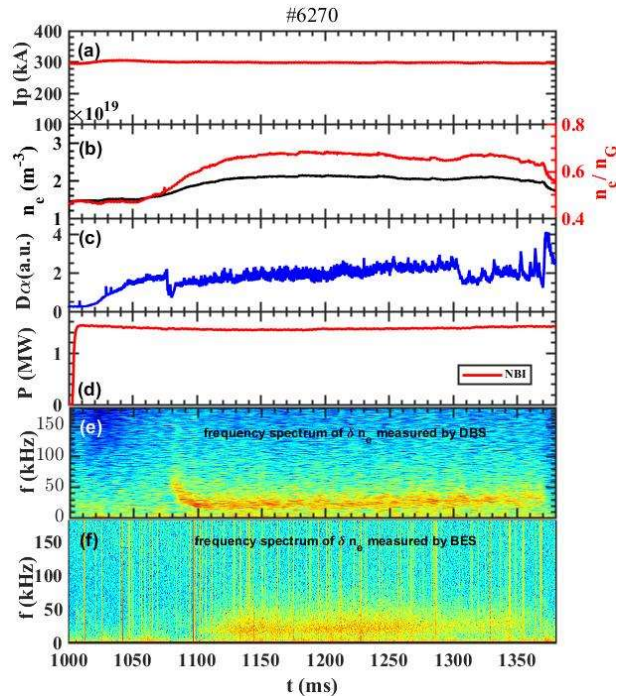


FIG. 3 The ELM-free regime in high density and high q_{95} : (a) plasma current, (b) line-averaged density, (c) divertor D_α emission, (d) NBI power, (e) frequency spectrum of density perturbation measured by DBS at the pedestal, (f) frequency spectrum of density perturbation measured by BES at the pedestal.

3.2. Small ELM regimes

Triangularity, density and q_{95} play an important role in achieving small ELMs on HL-3. There are large ELMs when operated in high upper-triangularity, medium density, and the small ELMs appear during the inter-large ELMs (large ELM mixed with small ELMs) with density increases when $\delta_u > 0.4$. Based on this mixed-ELM regime, it could be converted to small ELMs completely by two approaches, one way is to raise q_{95} (probably leading to grassy ELM), and another way is to raise density (probably leading to QCE). Fig. 3 shows the variations of ELM behaviors with different densities at large triangularity, it is shown that it is dominated by large ELMs in shot #6608 with middle density case, while small ELMs appear during the inter-large ELMs with the density in shot #6605 and #6606, finally, the large ELMs are replaced with the small ELMs mostly in shot 6603, which is high density discharge.

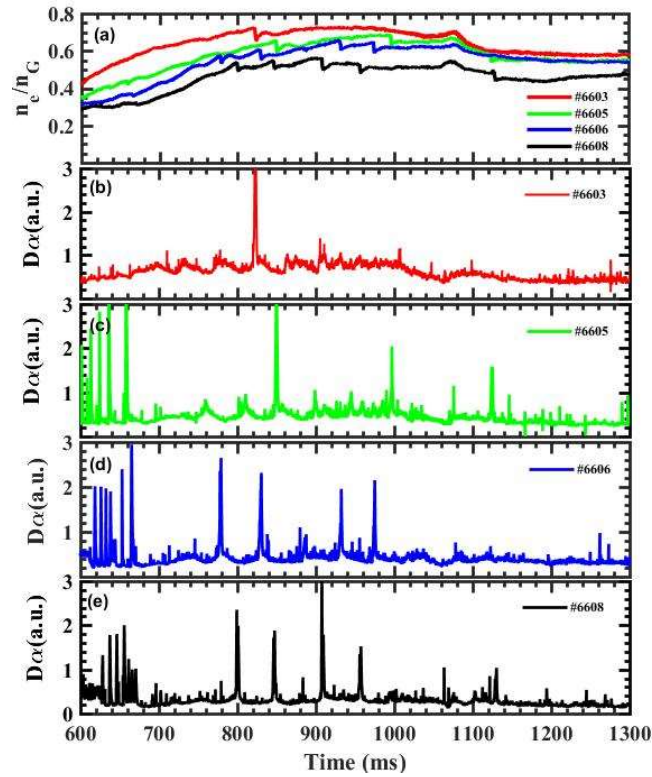


FIG. 4 The effect of density on ELM behaviors: (a) the normalized density of different shots, the corresponding divertor D_α for shots of #6603 (b), #6605 (c), #6606 (d), #6608 (e).

The details about the small ELMs for shot 6603 are displayed in Fig.5. the ELM frequency is hundreds of hertz, and the stored energy loss ratio induced by small ELMs decreased to $\delta W_{ELM}/W_E(\%) < 2\%$. One point should be noticed is that there is QCM with central frequency about 6 kHz during the duration of small ELMs from 600 ms to 1100 ms, which shows a stronger particle transport as shown by the divertor D_α , when the density decreases, the central frequency of QCM increases to about 13 kHz accompanied by the frequency spectrum width increases as well, but the particle transport decreases slightly. The results suggest that the QCM may play an important role in the small ELM regimes, similar to the QCE as observed in AUG[6, 7], which has a strong dependence on the triangularity and density, and is considered to be triggered by the resistive ballooning mode near the separatrix, and further physical analysis will be carried out. Both high $\beta_N \sim 2$ and confinement factor $H_{98} \sim 1.2$ have been achieved in this small ELMs, suggesting the promising application in future fusion reactors.

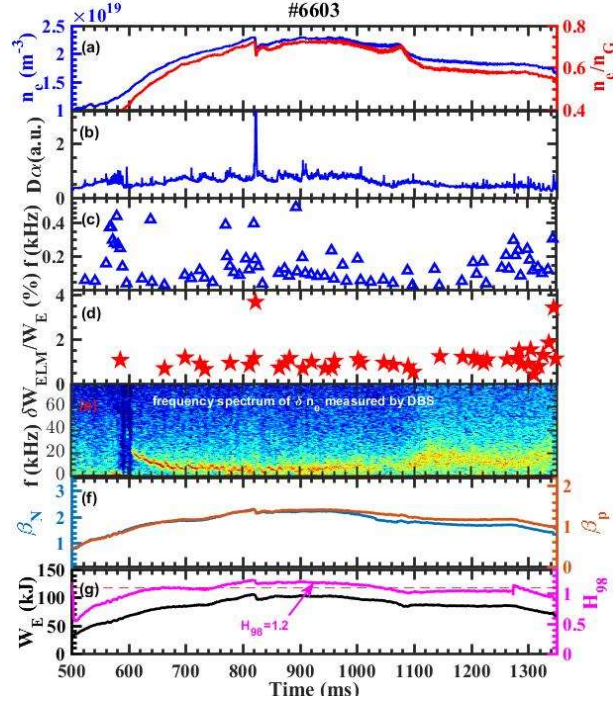


FIG. 5 The small regime in high β_N : (a) the central-line averaged density and normalized density by Greenwald density, (b) divertor D_α , (c) ELM frequency, (d) stored energy loss rate induced by ELMs, (e) frequency spectrum of density perturbation measured by DBS at the pedestal, (f) normalized beta and poloidal beta, (g) plasma stored energy and confinement factor H_{98} .

The statistical results suggests that the parameters of upper-triangularity δ_u , edge safe factor q_{95} and density n_e play an important role in achieving small ELMs based on the experiment performed in 2024 spring on HL-3. Fig. 6 provides the corresponding statistical law, and the colorbar represent the stored energy loss ratio $\delta W_{ELM}/W_E(\%)$ induced by ELMs. In general, the ELMs with $\delta W_{ELM}/W_E(\%) < 2\%$ are located in high density, high q_{95} and high triangularity parameter region, both the high density and high triangularity are important in achieving the small ELMs. High q_{95} favors the small ELMs, and the small ELMs could be obtained in medium q_{95} as well if the density and triangularity are large enough, but it is not enough to reduce the ELM amplitude only raise q_{95} in low triangularity.

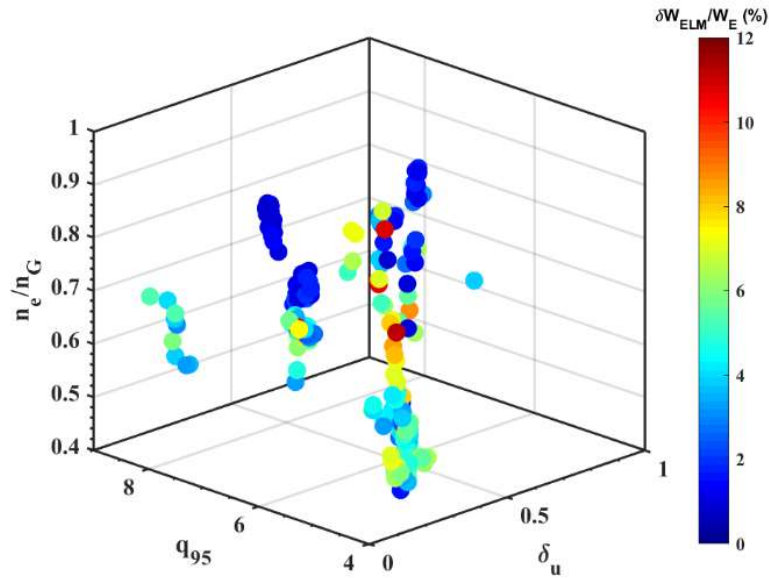


FIG. 6 The dependence of the stored energy loss induced by ELMs on upper-triangularity, q_{95} and density normalized by Greenwald limit.

Fig.7 shows that the regression analysis about the energy loss rate induced by ELM. The results provide the relationship between the energy loss rate induced by ELM $\delta W_{ELM}/W_E(\%)$ and plasma parameters, which show that $\delta W_{ELM}/W_E(\%)$ is inversely proportional to upper triangularity, q_{95} and normalized density, and it is consistent with the statistical results in Fig.6. While it increases with plasma current, toroidal magnetic field, normalized beta and poloidal beta, and this regression only include the $I_p=300$ kA-500 kA discharges in 2024 experiment, further statistical analysis will be performed to include more data in different discharge parameters.

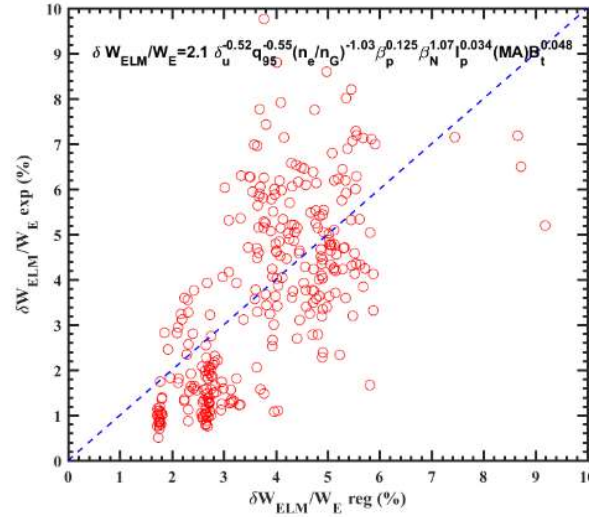


FIG. 7 Regressed analysis versus energy loss rate induced by ELM

4. SUMMARY

Several types of H-mode operation have been achieved with different current platforms ($I_p = 0.3 - 1.5$ MA) on HL-3, including ELM-free H-mode, type-I ELM, type-III ELM, small ELM (possible QCE, grassy ELM), and the ELM behavior shows a strong dependence on plasma parameters, such as triangularity, density, q_{95} , plasma beta and so on. High triangularity benefits the achievement of ELM-free, and there are two types of ELM-free regimes. One is dominated by electromagnetic coherent perturbation with frequency of about 50 kHz, which are observed on both Mirnov signal and the divertor saturation ion current, and they are coherent, suggesting that it is a large scale MHD, accompanied by weak particle transport, and this type of ELM-free usually occur in low q_{95} ; Another type of ELM-free is dominated by pedestal QCM with frequency of about 20 kHz, and it shows strong particle transport, which is helpful to the sustainment of ELM-free regime, high density and high q_{95} favors the achievement of this type of ELM-free in high triangularity. However, the physical characteristics of the coherent perturbation and QCM remain to be investigated. Small ELM (possible QCE) has been achievement by increasing density in high triangularity as well, and QCM with frequency of about 6-13 kHz has been measured by DBS, which may be the dominant reason of maintaining small ELMs. What is more, the statistical results show that the triangularity, density and q_{95} play an important role in reducing the energy loss ratio induced by ELM. HL-3 tokamak has the ability of high parameter operation, aiming to resolve the critical physics questions for future reactors, thus further exploration of small ELMs and ELM-free regimes with high parameters on HL-3 is necessary. In the future, we will focus on the two points: 1) The nature of the pedestal QCM and the underlying physics on the sustainment of ELM-free regimes; 2) The physical mechanism of small ELMs and its application in core-edge integration scheme for fusion reactors.

ACKNOWLEDGEMENTS

This work is supported by National Key R&D Program of China under Grant Nos. 2019YFE03030002, 2019YFE03090400, and National Natural Science Foundation of China under Grant Nos. 12475219, and Natural Science Foundation of Sichuan Province under Grant No. 2025ZNSFSC0066.

REFERENCES

- [1] Fenstermacher M. E. *et al* 2025 *Nuclear Fusion* **65** 053001
- [2] Oyama N. *et al* 2010 *Nuclear Fusion* **50** 064014

- [3] Xu G. S. *et al* 2019 *Phys. Rev. Lett.* **122** 255001
- [4] Saibene G. *et al* 2005 *Nuclear Fusion* **45** 297-317
- [5] Stober J. *et al* 2005 *Nuclear Fusion* **45** 1213-1223
- [6] Dunne M. *et al* 2024 *Nuclear Fusion* **64** 124003
- [7] Harrer G. F. *et al* 2022 *Phys. Rev. Lett.* **129** 165001
- [8] Maingi R. *et al* 2005 *Nuclear Fusion* **45** 264-270
- [9] Terry J. L. *et al* 2005 *Nuclear Fusion* **45** 1321-1327
- [10] Oyama N. *et al* 2005 *Nuclear Fusion* **45** 871–881
- [11] Gil L. *et al* 2025 *Nuclear Fusion* **65** 046002
- [12] Bernert M. *et al* 2020 *Nuclear Fusion* **61** 024001
- [13] Zhong W. *et al* 2024 *The Innovation* **5** 100555
- [14] Huang Z. H. *et al* 2025 *Nuclear Materials and Energy* **42** 101892